Scattering of a Gaussian Beam by an Ellipsoidal Particle with Vectorial Complex Ray Model

K. F. Ren
CORIA — UMR 6614, Normandie Université, CNRS, Université et INSA de Rouen
675 Av. de l'Université, BP 12, 76801 Saint Etienne du Rouvray, France

Abstract— By introducing the wave front curvature as a generic property of rays, the Vectorial Complex Rays Model (VCRM) improves considerably the precision of ray models. This has been already applied to the prediction of the scattering diagrams of the plane wave by large ellipsoidal particles and the two dimensional Gaussian beam scattering by an elliptical infinite cylinder at normal incidence. In this communication, the VCRM will be further extended to the scattering of a Gaussian beam by an ellipsoidal particle. The amplitude, the phase and the wave front curvature of the incident Gaussian beam are considered, but the diffraction has not been taken into account yet.

1. INTRODUCTION

The numerical prediction of the scattering properties of electromagnetic waves or light by objects of complex shape and of size much larger than the wavelength has been always a great challenge in both the field of electromagnetic computation or light interaction with particles. Among a large number of theories, models and algorithms, the methods based on the ray models seem to be the most appropriate due to their flexibility, their capability to deal with very large objects and their rapidity in term of the numerical calculation. But the precision is often not satisfactory because the wave properties (phase, divergence/convergence ...) are not properly taken into account.

In the model developed by the author — Vectorial Complex Rays Model (VCRM) [1, 2], the aforementioned wave properties are counted correctly by introducing the wave front curvature as a generic property of rays. Therefore, the VCRM improves considerably the precision of ray models. It has been validated by comparison with two rigorous methods: Lorenz-Mie theory for spherical particle [1–4] and the Multilevel Fast Multipole Algorithm (MLFMA) [5] for the ellipsoidal particles. It has been used to the prediction of the scattering diagrams of the plane wave by large ellipsoidal particles [6] and the elliptical infinite cylinders [7]. It has also been applied to the scattering of a two dimensional Gaussian beam by an elliptical infinite cylinder at normal incidence [8]. In this paper, we extend further the VCRM to the scattering of a Gaussian beam by an ellipsoidal particle. The amplitude, the phase and the wave front curvature of the incident Gaussian beam are considered in the model. But the diffraction has not yet taken into account. The results of the developed code will be compared with the rigorous Generalized Lorenz-Mie Theory (GLMT).

The rest of the paper is organized as follows. The Vectorial Complex Ray Model for the scattering of a Gaussian beam by an ellipsoidal particle is described in Section 2. The developed code is validated in Section 3 by comparison with the rigorous method, i.e., the Generalized Lorenz-Mie theory. The Section 4 is devoted to the presentation and the discussion of the numerical results. The last section is the conclusions.

2. VCRM FOR THE SCATTERING OF A GAUSSIAN BEAM

Consider an ellipsoidal particle of three semi-axes (a, b, c) respectively in (x, y, z) directions with the center located at O_P, the origin of the coordinate system O_p-xyz, referred hereafter as particle coordinate system. The particle is illuminated by a Gaussian beam of waist radius w_0 propagating in its coordinate system $O_b(u, v, w)$ along w axis which make an angle θ_0 with z axis. The coordinates of the beam center O_b in the particle coordinate system are (x_0, y_0, z_0) (Fig. 1). For simplicity, in this paper, we suppose that the beam axis is in a symmetric plane of the ellipsoid. Without lose of generality, we choose the plane $(O_P$-$xy)$. The observation is also limited in (x, z) plane, so that all rays under study remain in the same plane and we have $\phi = 0$ and $y_0 = 0$ in the case under study.

In the VCRM, each ray possesses five properties: the direction, the amplitude, the phase, the polarization and the wave front of the wave the ray represents. All these properties evolve each time a ray interacts with the particle surface and can be calculated step by step according to the standard procedure of the VCRM as described in [1, 2] and [3, 4]. It is worth, however, to note that in the VCRM, the wave vector, as well as its normal and tangent components to the particle surface,

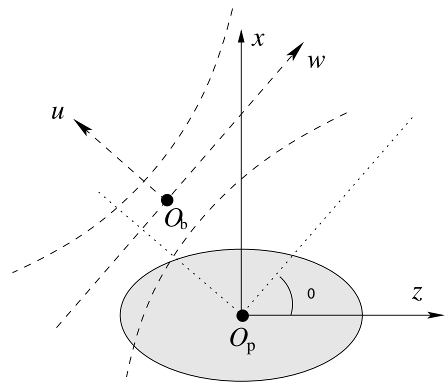

Figure 1: Definition of the coordinate systems.

are used for the determination of the propagation direction (after a reflection or a refraction) and the Fresnel coefficients. This simplifies significantly the ray tracing, especially in three dimension scattering. The divergence and the convergence of the wave on the surface of the particle are predicted directly by the wave front curvature, the latter permits also determining the phase due to the focal lines by counting the number of changes of sign of the wave front curvature radii. The reader are refereed to the references cited above for the details.

The difference of the VCRM for the plane wave and for a focused beam lies in the wave front shape before the first interaction of a ray with the particle and the variation of the incident wave amplitude. We will give a detailed description in the following.

The complex amplitude (with time convention $e^{i\omega t}$) of a Gaussian beam is written as

$$S_G(u,v,w) = A_G \exp(-i\Phi)$$

where A_G and Φ present respectively the amplitude and the phase of the beam and are given by

$$A_G = \frac{w_0}{w_l} \exp\left(-\frac{u^2+v^2}{w_l^2}\right) \tag{1}$$

and

$$\Phi(u,v,w) = k\left\{w + \frac{u^2+v^2}{2w[1+(z_R/w)^2]}\right\} + \tan^{-1}\left(\frac{w}{z_R}\right) \tag{2}$$

k is the wave number and z_R is the Rayleigh length defined by

$$z_R = \pi w_0^2/\lambda \tag{3}$$

w_l is the local radius of the beam at w and is related to the beam waist radius w_0 by

$$w_l = w_0\left[1+(w/z_R)^2\right]^{1/2} \tag{4}$$

To calculate the amplitude and the phase of the incident beam at the point where the ray interacts with the particle, we use the following relations between the particle coordinate system O_p-xyz and the beam coordinate system O_b-uvw given by

$$u = (x-x_0)\cos\theta_0 - (z-z_0)\sin\theta_0 \tag{5}$$
$$w = (x-x_0)\sin\theta_0 + (z-z_0)\cos\theta_0 \tag{6}$$

with $v = 0$ since the beam axis and the observation are in the plane O_P-xz.

To ensure that a ray interacts with the surface of the particle, we calculate the scalar product of the wave vector and the outward normal of the particle surface. If the result is negative the ray interacts with the particle and then we calculate the Fresnel coefficients for the two polarizations; the directions, the phase and the wave front curvatures of the reflected and the refracted rays. Then we determine the following interaction point according to the direction of the refracted ray and the equation describing the surface of the particle. We repeat the similar procedure as for the first interaction so that to determine the properties of the emergent ray and the internal reflected ray, until a order for which the amplitude of the ray is negligible. Finally, we should calculate the summation of the complex amplitudes of all emergent rays to obtain the scattering diagram.

3. VALIDATION OF THE CODE

In order to validate the code we compare firstly the scattering diagrams calculated by the VCRM and the GLMT for a spherical particle of radius $a = 30\,\mu\text{m}$ and the refractive index $m = 1.333$ located at the center of a Gaussian beam of wavelength $\lambda = 0.6328\,\mu\text{m}$ with two different beam waists. We found that when the beam waist radius is relatively large compared to the particle size, i.e., $w_0 = 100\,\mu\text{m}$ (Fig. 2, the scattering diagrams are similar to those of a plane wave). The agreement between the two methods is good except in the two regions. one is the narrow region in forward direction, this is because the diffraction has not been taken into account. The other is in the Alexander region (between the first and the second rainbows), this is to be improved by taken into account the diffraction effect in the caustic regions.

When the beam waist radius is much less than the particle radius, i.e., $w_0 = 10\,\mu\text{m}$ (Fig. 3), the scattering diagrams of the VCRM agree almost perfectly in all directions for the two polarizations. The reason of the discrepancy in forward direction (scattering angle smaller than about $5°$) is the same as in Fig. 2. The disappearance of the disagreement around the Alexander region is due to the fact that the beam amplitude at the impact points of rainbow is much less than that near the beam axis. When the particle is illuminated with the same beam but off-axis, this effect may reappear (see the following section).

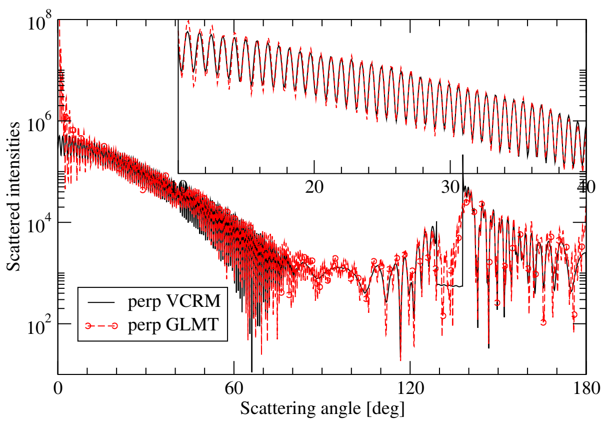

Figure 2: Comparison of the scattered diagrams calculated by VCRM abd GLMT for a spherical particle of radius $a = 30\,\mu\text{m}$, refractive index $m = 1.333$ illuminated by a Gaussian beam of wavelength $\lambda = 0.6328\,\mu\text{m}$ and beam waist radius $w_0 = 100\,\mu\text{m}$.

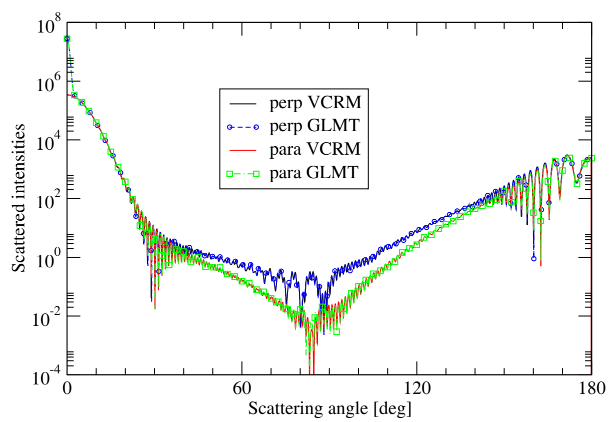

Figure 3: Comparison of the scattered diagrams calculated by VCRM and GLMT for the same parameters as in Fig. 2 except $w_0 = 10\,\mu\text{m}$.

4. NUMERICAL RESULTS AND DISCUSSION

We present in this section some typical scattering diagrams of an ellipsoidal particle illuminated by a Gaussian beam. Fig. 4 show the scattering diagrams of a particle of three different shape illuminated by an off-axis Gaussian beam. The wavelength of the incident Gaussian beam is still $0.6328\,\mu\text{m}$, its waist radius is $50\,\mu\text{m}$ and its center is located at $x_0 = 30\,\mu\text{m}$, $y_0 = z_0 = 0$. The polarization for the four curves is perpendicular, i.e., the incident electric field is in y direction. The black (solid line without symbol) and the red (dashed line) curves present respectively the results calculated by the GLMT and the VCRM. Similar remarks as in the last section can be made for the comparison of these two curves, but we found a dissymmetry of the scattering diagrams due to the off-axis of the incident beam. Furthermore, the second rainbow on the left (around $-125°$) is much less remarkable.

The other two curves in Fig. 4 are respectively the scattering diagrams of an oblate ($c = 45\,\mu\text{m}$, green curve with circles) and a prolate ($c = 55\,\mu\text{m}$, blue curve with diamond symbols) with the same cross circular section ($a = b = 50\,\mu\text{m}$). For clarity, these two curves are off-set respectively by 10^2 and 10^3. We may note that the profiles of the scattering diagrams between $-60°$ and $120°$ are similar to that of the sphere, while the structure of the diagrams around rainbow angles and in the backward direction are very sensible to the shape of the particle. The position of the first rainbow on the left of the figure moves about $+10°$ for the oblate and $-10°$ for the prolate relative to that of the sphere. In the other side the first and the second rainbows are merged for the oblate particle but very significant for the prolate particle. The Alexander region is also enlarged from 8° for the sphere to about 22° for the prolate particle.

At last, we present the scattering diagrams calculated by the VCRM in the most general case: an ellipsoidal particle with different semi-axes illuminated by an off-axis Gaussian beam with an incident angle. It can be noted that the scattering diagram around the rainbows is very sensible to the shape of the particle.

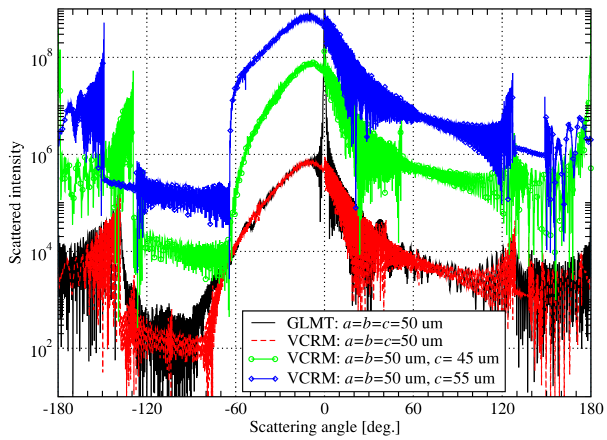

Figure 4: Scattering diagrams of particles with the same circular cross section ($a = b = 50\,\mu$m) illuminated by an off-axis ($x_0 = 30\,\mu$m) Gaussian beam ($\lambda = 0.6328\,\mu$m and $w_0 = 50\,\mu$m). The incident beam propagates in z direction and its electric field is polarized in y direction. For clarity, the curves for the oblate in green and that for the prolate in blue are off-set respectively by 10^2 and 10^3.

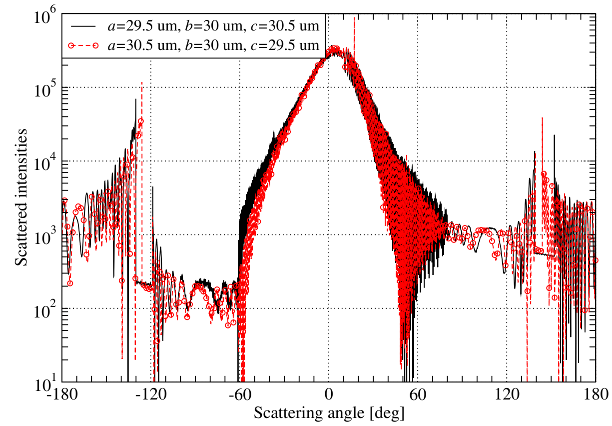

Figure 5: Scattering diagrams of an ellipsoidal particle with different semi-axes a, b and c of water $m = 1.333$ illuminated by a Gaussian beam of wavelength $\lambda = 0.6328\,\mu$m and waist radius $w_0 = 30\,\mu$m. The beam axis is in the xz plane and makes an angle of 10° with z axis. The beam center is at (10 µm, 0, 0) in the particle coordinate system.

5. CONCLUSIONS

We have applied in this paper the Vectorial Ray Tracing Model for the calculation of the scattering diagrams of a large ellipsoidal particle. The code is first validated by comparison with the rigorous solution of Maxwell equations, i.e., the generalized Lorenz-Mie theory. The comparison showed that the VCRM permits to predict correctly the scattering diagram in almost all directions except in the Alexander region. The code is then applied to the prediction of the scattering diagrams of ellipsoidal water droplets with different semi-axis illuminated by a Gaussian beam in the on-axis and off-axis cases with the propagation direction along a symmetric axis of the particle or with an incident angle. It is shown that the rainbow positions and its structure are very sensible to the position as well as the shape of the particle. This dependence may provide very useful information for the measurements of the non-spherical particle, especially in the two phase flows.

ACKNOWLEDGMENT

This work has been supported by the French National Agency under the grant number ANR-13-BS09-0008-01 (AMOCOPS).

REFERENCES

1. Ren, K. F., F. Onofri, C. Rozé, and T. Girasole, "Vectorial extended geometrical optics for scattering of a spheroid," *Progress In Electromagnetics Research Symposium Abstracts*, 145, Cambridge, USA, July 5–8, 2010.
2. Ren, K. F., F. Onofri, C. Rozé, and T. Girasole, "Vectorial complex ray model and application to twodimensional scattering of plane wave by a spheroidal particle," *Opt. Lett.*, Vol. 36, No. 3, 370–372, 2011.
3. Yuan, Y., "Diffusion de la lumière par un objet irrégulier pour lapplication à limagerie des sprays," PhD Thesis, Rouen University, France, 2012.
4. Jiang, K., "Theoretical study of light scattering by an elliptical cylinder," PhD Thesis, Rouen University, 2013.

5. Yang, M., Y. Wu, X. Sheng, and K. F. Ren, "Comparison of scattering diagrams of large non-spherical particles calculated by VCRM and MLFMA," *J. Quant. Spect. Rad. Trans.*, Vol. 156, 88–96, 2015.
6. Ren, K. F., C. Rozé, and T. Girasole, "Scattering and transversal divergence of an ellipsoidal particle by using vectorial complex raymodel," *J. Quant. Spectrosc. Radiat. Transfer*, Vol. 113, 2419–2423, 2012.
7. Jiang, K., X. Han, and K. F. Ren, "Scattering from an elliptical cylinder by using the vectorial complex ray model," *Appl. Opt.*, Vol. 51, No. 34, 8159–8168, 2012.
8. Jiang, K., X. Han, and K. F. Ren, "Scattering of a gaussian beam by an elliptical cylinder using the vectorial complex ray model," *J. Opt. Soc. Am. A*, Vol. 8, 1548–1556, 2013.